# SANDIA REPORT

SAND2013-3429
Unlimited Release
Printed April, 2013

# Probability Distribution of von Mises Stress in the Presence of Pre-Load

Daniel J. Segalman, Richard V. Field, Jr., and Garth M. Reese

Prepared by
Sandia National Laboratories
Albuquerque, New Mexico 87185 and Livermore, California 94550

Sandia National Laboratories is a multi-program laboratory managed and operated by Sandia Corporation, a wholly owned subsidiary of Lockheed Martin Corporation, for the U.S. Department of Energy's National Nuclear Security Administration under contract DE-AC04-94AL85000.



Sandia National Laboratories

Issued by Sandia National Laboratories, operated for the United States Department of Energy by Sandia Corporation.



Available to DOE and DOE contractors from
U.S. Department of Energy
Office of Scientific and Technical Information
P.O. Box 62
Oak Ridge, TN 37831

Telephone: (865) 576-8401
Facsimile: (865) 576-5728
E-Mail: reports@adonis.osti.gov
Online ordering: http://www.osti.gov/bridge

Available to the public from
U.S. Department of Commerce
National Technical Information Service
5285 Port Royal Rd
Springfield, VA 22161

Telephone: (800) 553-6847
Facsimile: (703) 605-6900
E-Mail: orders@ntis.fedworld.gov
Online ordering: http://www.ntis.gov/help/ordermethods.asp?loc=7-4-0#online

SAND2013-3429
Unlimited Release
Printed April, 2013

# Probability Distribution of von Mises Stress in the Presence of Pre-Load

Daniel J. Segalman
Multi-Physics Modeling Simulation
Sandia National Laboratories
Livermore, CA 94551-0969
djsegal@sandia.gov

Richard V. Field, Jr.
Component Science & Mechanics
Sandia National Laboratories
Albuquerque, NM 87185-0346
rvfield@sandia.gov

Garth M. Reese
Computational Solid Mechanics and Structural Dynamics
Sandia National Laboratories
Albuquerque, NM 87185-0380
gmreese@sandia.gov

**Abstract**

Random vibration under preload is important in multiple endeavors, including those involving launch and re-entry. There are some methods in the literature to begin to address this problem, but there is nothing that accommodates the existence of preloads and the necessity of making probabilistic statements about the stress levels likely to be encountered. An approach to achieve to this goal is presented along with several simple illustrations.

# Acknowledgments

The first author thanks his wife for permitting him to put off travel during the winter shutdown in order to do the work presented here. The authors also express our appreciation to David Day, also of Sandia National Laboratories, for very helpful mathematical discussion about an approximation used in this work.

# Contents



## Appendix

# Figures



# Tables

# Nomenclature

$\beta(t)$ $X^{-1}Q^T q(t)$, page 15

$\gamma$ $G(x)\,\sigma_0(x)$, page 17

$\Gamma_{qq}$ The zero-time lag covariance matrix of modal displacement: $E\left[qq^T\right]$, page 14

$\hat{q}(t)$ $Q\,X\,\beta(t)$, page 15

$\mathcal{R}^d$ The $d$-dimensional space of real numbers, page 11

$\Psi(x)$ Matrix each of whose columns is the vector of stress components associated with that mode at that location (modal stresses), page 13

$\Psi_n(x)$ The $n^{th}$ column of $\Psi(x)$, page 13

$\rho_B$ Density of beam in first and second example problems, page 24

$\sigma(x,t)$ Instantaneous stress at location $x$ and time $t$, page 13

$\sigma_0(x)$ Static stress at location $x$, page 13

$A$ 6x6 matrix mapping used to map stress vectors to von Mises stress, page 14

$B(x)$ $\Psi^T(x)\,A\,\Psi(x)$, page 14

$C$ $X\,Q^T\,B\,Q\,X$, page 15

$d$ The number of applied random dynamic forces, page 11

$D(x)$ Defined in decomposition $C(x) = R(x)\,D^2(x)\,R^T(x)$, page 15

$F_0$ Vector of static loads applied to structure, page 11

$G$ $-D^{-2}\,R^T\,X^T\,Q^T\,\Psi^T\,A$, page 17

$L$ Length of beam in first and second example problems, page 24

$N_M$ The number of vibration modes retained for analysis, page 13

$N_P$ The number of stress processes, page 15

$N_R$ The rank of $\Gamma_{qq}$, page 14

$p(x,t)$ von Mises stress at location $x$ and time $t$, page 14

$p^2_{\text{RMS}}$ time average of the square of von Mises stress, page 14

$Q$ Element of decomposition $\Gamma_{qq} = Q\,X Q^T$, page 14

$R(x)$ Defined in decomposition $C(x) = R(x)\,D^2(x)\,R^T(x)$, page 15

$S_{qq}$ cross spectral density matrix of modal displacements, page 11

$w$ Half width of beam in first and second example problems, page 24

$X$ Element of decomposition $\Gamma_{qq} = Q\,X Q^T$, page 14

$y(t,x)$ $R^T(x)\,\beta(t)$, page 16

$Y_0^2$ $p_0^2 - \gamma^T\,D^2\,\gamma$, page 17

CDF Cumulative Distribution Function, page 29

F(t) Vector of random dynamic loads applied to structure, page 11

PDF Probability Density Function, page 29

q(t) Column vector of modal displacements, page 13

# 1 Introduction

Random vibration under preload is important in multiple endeavors, including those involving launch and re-entry. In these days of increasing reliance on predictive simulation, it is important to address this problem in a probabilistic manner - this is the appropriate flavor of quantification of margins and uncertainties in the context of random vibration. There are some methods in the literature that only begin to address this problem:

1. Miles' [3] equation addresses the accelerations seen by a single degree of freedom system supported by a randomly driven base. The attachment stresses are presumed to be proportional to the relative displacements. This is, of course, not suitable for real physical systems containing multiple degrees of freedom.

2. A method of Segalman et. al. [6] facilitates estimating the RMS value of von Mises stresses under pre-load for arbitrary weakly stationary random dynamic loads, so long as the cross-spectral density matrix for load is available. This says nothing about probability distribution of von Mises stress.

3. Another method of Segalman et. al. [7] does provide a method for calculating the probability distribution of von Mises stress so long as the applied random dynamic loads are stationary Gaussian and there is no pre-load.

4. Tibbits [8] extended the method of [7] to the case where there is pre-load, but where only one random dynamic stress load is applied. Though a major advance, this still does not admit re-entry type cases - where non-uniform random dynamic loads are distributed spatially about the structure.

None of these methods can be employed to address the severe conditions of random vibration applied to a structure also subject to preload - for which launch or re-entry would be paradigms - and generate probabilistic expressions for the von Mises stress likely to be encountered.

It is the purpose of this monograph to present such a method.

# 2 Key Ingredients

The most important ingredient to this development is the partition of the applied loads into a system of random dynamic loads $F(t)$ and a set of static pre-loads $F^0$. One might assume that the static loads are self-equilibrating, but the following development does not require that condition. Also, critical to the following development is the assumption that the random dynamic load components are stationary Gaussian with zero mean.

Let $F(t)$ be an $\mathcal{R}^d$-valued, weakly stationary Gaussian process of zero mean and having correlation matrix $r_{FF}(\tau) = E\left[F(t)\,F(t+\tau)^T\right]$, a $d$x$d$ matrix. The matrix of two-sided spectral densities [5] is denoted by $S_{FF}(\omega)$ [5]

$$S_{FF}(\omega) = \frac{1}{2\pi}\int_{\mathcal{R}} r_{FF}(\tau)\, e^{-i\omega\tau}\, d\tau. \tag{2.1}$$

This matrix defines the characterization of the input needed for random vibration studies.

From $S_{FF}(\omega)$ plus the structure's frequency response functions we can derive the cross spectral density matrix of modal displacement $S_{qq}(\omega)$. From $S_{qq}(\omega)$ we can evaluate the $\Gamma_{qq}$, the zero-time lag covariance matrix of modal displacement. ($\Gamma_{qq}$ is defined mathematically below.)

All of the above operations are defined in the Appendix. In the following section, we show how knowing $\Gamma_{qq}$ and assuming that all loads are Gaussian processes, we may determine the statistics of von Mises stress, even in the presence of pre-load.

# 3 Separation of Stress Response due to Static and Random Vibration Loads

At each location $x$ in the structure, we can express the stress vector (discussed more below) in terms of modal displacements

$$\sigma(t,x) = \sigma_0(x) + \sum_n q_n(t)\,\Psi_n(x) = \sigma_0(x) + \Psi(x)\,q(t), \tag{3.1}$$

where $q$ is a column vector of modal displacements with coordinates $q_n$ and $\Psi(x)$ is a matrix each of whose columns is the vector of stress components associated with that mode at that location (modal stresses). Vector $\Psi_n(x)$ is the $n^{th}$ column of $\Psi(x)$. We have truncated the sum at $N_M$ modes.

The square of the von Mises stress is

$$p^2(t,x) = \Big(\Psi(x)q(t) \,+\, \sigma_0(x)\Big)^T\, A\,\Big(\Psi(x)q(t) \,+\, \sigma_0(x)\Big), \tag{3.2}$$

where

$$A = \begin{bmatrix} 1 & -1/2 & -1/2 & 0 & 0 & 0 \\ -1/2 & 1 & -1/2 & 0 & 0 & 0 \\ -1/2 & -1/2 & 1 & 0 & 0 & 0 \\ 0 & 0 & 0 & 3 & 0 & 0 \\ 0 & 0 & 0 & 0 & 3 & 0 \\ 0 & 0 & 0 & 0 & 0 & 3 \end{bmatrix} \tag{3.3}$$

We expand the argument in Equation 3.2:

$$\begin{aligned} p^2(t,x) = \Big(\Psi(x)\,q(t)\Big)^T\, A\,\Big(\Psi(x)\,q(t)\Big) + \sigma_0^T(x)\,A\,\sigma_0(x) \\ + \Big(\Psi(x)\,q(t)\Big)^T\, A\,\sigma_0(x) + \sigma_0^T(x)\,A\,\Big(\Psi(t)\,q(t)\Big). \end{aligned} \tag{3.4}$$

Let $p_R^2(t,x)$ denote the component of squared von Mises stress due solely to random vibration, that is, the first term on the LHS of Equation 3.4. Then

$$p_R^2(t,x) = \Big(\Psi(x)\,q(t)\Big)^T\, A\,\Big(\Psi(x)\,q(t)\Big) = q(t)^T\,B(x)\,q(t), \tag{3.5}$$

where

$$B(x) = \Psi^T(x)\,A\,\Psi(x). \tag{3.6}$$

It follows that

$$E[p_R^2(t,x)] = B(x)_{ij}E[q_iq_j] = B(x)_{ij}\Big(\Gamma_{qq}\Big)_{ij} = \Big(B(x)^T\Gamma_{qq}\Big)_{jj} = \mathrm{Tr}\,\Big(B^T(x)\,\Gamma_{qq}\Big) \tag{3.7}$$

where

$$\Gamma_{qq} = E[q(t)\, q^T(t)] \tag{3.8}$$

is the zero-time lag covariance matrix of modal displacement. We note that $\Gamma_{qq}$ has neither spatial or temporal dependence and that $B$ has spatial dependence only. Also both matrices are symmetric, so the use of $()^T$ in Equation 3.7 is optional.

## 3.1 An intermediate result: RMS von Mises

Let's take the expected value of both sides of Equation 3.4 to find

$$p^2_{\text{RMS}}(x) = E\left[p^2(t,x)\right] = E\left[q^T(t)\, B(x)\, q(t)\right] + 2\, E\left[q^T(t)\right] \Psi^T(x)\, A\sigma_0(x) + \sigma_0^T(x)\, A\, \sigma_0(x), \tag{3.9}$$

but $E[q] = 0$, so the difference between the square of RMS von Mises stress in the absence of pre-stress (Equation 3.7) and the square of von Mises stress in the presence of pre-stress (Equation 3.9) is the square of von Mises stress of the pre-load alone ($\sigma_0^T A\sigma_0$). Examining the un-squared von Mises stress, we see that

$$p_{\text{RMS}}(x) = \sqrt{\text{Tr}\left(B^T(x)\,\Gamma_{qq}\right) + \sigma_0^T(x)\, A\, \sigma_0(x)} \leq \sqrt{\text{Tr}\left(B^T(x)\,\Gamma_{qq}\right)} + \sqrt{\sigma_0^T(x)\, A\, \sigma_0(x)}. \tag{3.10}$$

Hence, the RMS von Mises stress is less than or equal to the sum of that due to random vibration and that due to preload.

## 3.2 Reduction to Stress Processes

Noting that matrix $\Gamma_{qq}$ is square ($N_M$x$N_M$) and positive semi-definite, we may decompose it

$$\Gamma_{qq} = Q\, X^2\, Q^T, \tag{3.11}$$

where $X$ is a diagonal matrix whose dimension ($N_R$) is the rank of $\Gamma_{qq}$ and $Q$ is a rectangular matrix having the property that

$$Q^T\, Q = I_{N_R} \tag{3.12}$$

where $I_{N_R}$ is the identity matrix of rank $N_R$. Note that because $\Gamma_{qq}$ has no time or spatial dependence, neither do $Q$ or $X$.

This permits us a change of variables

$$\beta(t) = X^{-1} Q^T q(t) \tag{3.13}$$

where, by construction,

$$E[\beta(t)\,\beta(t)^T] = I_{N_R} \tag{3.14}$$

so that the elements of $\beta$ are independent, identically distributed random processes. (Proof of this requires that we recall that $X$ is a diagonal matrix.) While $Q$ is not generally invertible, we may introduce the new random vector

$$\hat{q}(t) = Q\,X\,\beta(t). \tag{3.15}$$

It is shown in Appendix B that $q$ and $\hat{q}$ have identical first and second moments, and are therefore equivalent Gaussian random vectors. For the purpose of characterizing the statistics of von Mises stress, we could employ $\hat{q}$ in Equation 3.4 with the same legitimacy as employing $q$.

In our new coordinates $\beta$, the square of the von Mises stress *due solely to random vibration* is

$$p_R^2(t,x) = \beta^T(t)\,C(x)\,\beta(t), \tag{3.16}$$

where

$$C(x) = X^T\,Q^T\,B(x)\,Q\,X. \tag{3.17}$$

Matrix $C(x)$ is square, having dimensionality equal to the rank of $\Gamma_{qq}$ but possibly much lower rank. The rank of $C$ is the minimum of the rank of the matrices in the product on the right hand side of Eq. 3.17. Note that $\text{rank}(X) = \text{dimension}(X) = \text{rank}(\Gamma_{qq}) = N_R$ and $\text{rank}(B) \leq \text{rank}(A) = 5$.

We exploit the symmetry and the positive semi-definiteness of $C(x)$ in doing its singular value decomposition:

$$C(x) = R(x)\,D^2(x)\,R^T(x), \tag{3.18}$$

where the matrix $D(x)$ is diagonal and has dimension equal to the rank of $N_P$ of $C(x)$, $R(x)$ is a rectangular matrix having property that $R^T R = I_{C(x)}$, and $I_{C(x)}$ is the identity matrix whose dimension is the rank of $C(x)$. We refer to $N_P$ as the number of stress processes.

The square of the von Mises stress due solely to random vibration is now

$$p_R^2(t,x) = \beta^T(t)\,R(x)\,D^2(x)\,R^T(x)\,\beta(t). \tag{3.19}$$

This suggests yet another change of variables:

$$y(t,x) = R^T(x)\,\beta(t). \tag{3.20}$$

It is easily shown that the elements of y are independent, identically distributed (IID) Gaussian processes with unit variance. (This again employs the fact that $X$ is a diagonal matrix.) There are two obvious advantages of the above transformation: (1) it reduces the number of

random variables of this problem to the rank of A (at most 5), and (2) it aligns the random variables in the directions of the axes of the ellipsoids of constant von Mises stress.

When Equation 3.20 is substituted into Equation 3.19, we obtain

$$p_R^2(t,x) = y(t,x)^T\, D(x)^2\, y(t,x) = \sum_n y_n(t,x)^2\, D_n(x)^2. \tag{3.21}$$

The above expression suggests the following terminology. We refer to the dimension of $D(x)$ as the number of independent 'stress processes' acting at the location $x$.

It is worthwhile to discuss how many modes should be retained in the above calculations. As in other cases of modal synthesis, one must include those modes whose frequency response functions significantly intersect the excitation spectrum. A conservative approach is to employ all modes through an upper bound of the frequencies in the power spectrum of the input loads. Since the largest computational effort involves the decomposition in Eq. 3.11, and that need be done only once per load case, the cost of such conservatism is not unreasonable.

Let us now return to calculation of the full von Mises stress, as presented in Equation 3.4, but with our newer degrees of freedom, that is,

$$p^2(t,x) = y(t,x)^T\, D^2(x)\, y(t,x) + 2\,\beta(t)^T \Big( X^T\, Q^T\, \Psi(x)^T \Big)\, A\, \sigma_0(x) + \sigma_0(x)^T\, A\, \sigma_0(x). \tag{3.22}$$

Approximating[1]

$$\beta(t) \approx R(x) y(t,x) \tag{3.23}$$

at this location, we have

$$p^2(t,x) = y^T(t)\, D(x)^2\, y(t) + 2\, y(t)^T \Big( R(x)^T\, X\, Q^T\, \Psi(x)^T \Big)\, A\, \sigma_0(x) + \sigma_0(x)^T\, A\, \sigma_0(x). \tag{3.24}$$

Defining a vector $\gamma(x)$ by

$$\gamma(x) = G(x)\, \sigma_0(x), \tag{3.25}$$

where

$$G(x) = -D(x)^{-2}\, R(x)^T\, X\, Q^T\, \Psi(x)^T\, A \tag{3.26}$$

and $p_0^2(x) = \sigma_0^T(x) A \sigma_0(x)$, Equation 3.24 becomes

$$p^2(t,x) = y^T(t)\, D(x)^2\, y(t) - 2\, y(t)^T\, D(x)^2\, \gamma(x) + p_0(x)^2. \tag{3.27}$$

Obviously, this calls for completing the square

$$p^2(t,x) = (y(t) - \gamma(x))^T\, D(x)^2\, (y(t) - \gamma(x)) + Y_0(x)^2 \tag{3.28}$$

[1]By this approximation, we mean that $y(t,x)^T \Big( R(x)^T\, X\, Q^T\, \Psi(x)^T \Big)\, A$ and $\beta(t)^T \Big( X\, Q^T\, \Psi(x)^T \Big)\, A$ are statistically equivalent random vectors.

where

$$Y_0(x)^2 = p_0(x)^2 - \gamma(x)^T\, D(x)^2\, \gamma(x). \tag{3.29}$$

It appears that if $\sigma_0(x)$ is in the span of the vectors of $\Psi(x)$, $Y_0(x) = 0$. Otherwise $Y_0(x) > 0$.

The dimensions of the above matrices are presented in Tables 3.1 and 3.2. The dimensions themselves are discussed in Table 3.3.

Table 3.1: Global Matrices

| | $\Gamma_{qq}$ | $X$ | $Q$ | $A$ |
|---|---|---|---|---|
| Dimension | $N_M \times N_M$ | $N_R \times N_R$ | $N_M \times N_R$ | $6 \times 6$ |
| Character | | Diag. | | Rank 5 |

Table 3.2: Local Matrices

| | $\Psi$ | $B$ | $C$ | $D$ | $R$ | $G$ | $\gamma$ |
|---|---|---|---|---|---|---|---|
| Dimension | $6 \times N_M$ | $N_M \times N_M$ | $N_R \times N_R$ | $N_P \times N_P$ | $N_R \times N_P$ | $N_P \times 6$ | $N_P \times 1$ |
| Character | | | | Diag. | | | |

Table 3.3: Dimensions

| | |
|---|---|
| $N_M$ | Number of modes employed |
| $N_R$ | Rank of $\Gamma_{qq}$. $N_R \leq N_M$ |
| $N_P$ | Rank of $C$ = number of random stress processes. $N_P \leq \text{rank}(A) = 5$ |

# 4 Probabilistic Statements on von Mises Stress

The statistics of the von Mises stress are determined via appropriate integration over the joint probability distribution of the $y_k$'s defined by Equation 3.20.

## 4.1 A Previous Result from New Perspective

For instance we re-examine the mean square of the von Mises stress

$$\begin{aligned} E[p^2(t,x)] &= \int_{-\infty}^{\infty} \cdots \int_{-\infty}^{\infty} p^2(t,x) \prod_r \rho_r(y_r)\, \mathrm{d}y_r \\ &= \int_{-\infty}^{\infty} \cdots \int_{-\infty}^{\infty} \left( (y(t)-\gamma(x))^T D(x)^2 (y(t)-\gamma(x)) + Y_0(x)^2 \right) \prod_r \rho_r(y_r)\, \mathrm{d}y_r \\ &= \mathrm{Tr}(D(x)^2) + p_0(x)^2, \end{aligned} \tag{4.1}$$

where

$$\rho_r(y_r) = \frac{1}{\sqrt{2\pi}} e^{-y_r^2/2} \tag{4.2}$$

are the probability density functions of a standard Gaussian random variable. For more detail on this derivation, please refer to Appendix C. We see that $D_r(x)^2$ is the contribution of the $r^{th}$ random process to $E[p(t,x)^2]$ at location $x$ and the rank of $D$ is the number of independent random processes contributing to the von Mises stress response at that location.

## 4.2 Probability Distributions of von Mises Stress

To determine the probability law for $p(x,t)$, it is useful to work with the square of the von Mises stress. Further, because von Mises stress is non-negative, it follows that for any $Y$, we have $P(p \le Y) = P(p^2 \le Y^2)$. The probability that the square of von Mises stress amplitude is less than or equal to a quantity $Y^2$ is

$$F_Y = P(p^2 \le Y^2) = \begin{cases} 0 & \text{for} \quad Y \le Y_0 \\ \displaystyle\int_{Z(\{D\},\gamma,Y_0,Y)} \prod \rho_r(y_r) dy_r & \text{for} \quad Y > Y_0 \end{cases} \tag{4.3}$$

where $Z(\{D\},\gamma,Y_0,Y)$ is the $N_P$-dimensional ellipsoid containing points $y$ associated with the square of the von Mises stress less than or equal to $Y^2$, that is

$$Z(\{D\},\gamma,Y_0,Y) = \left\{ y : ((y-\gamma)^T D^2 (y-\gamma)) \le Y^2 - Y_0^2 \right\} \tag{4.4}$$

and $N_P$ is the rank of matrix $D$. Note that all the arguments of $Z$ are functions of $x$ only and that $Z(\{D\}, \gamma, Y_0, Y)$ is an ellipsoid centered at $\gamma$. The semi-axes of these ellipsoids are

$$A_r = \sqrt{\frac{Y^2 - Y_0^2}{D_r^2}} \tag{4.5}$$

See Figure 4.1. (It is because von Mises stress is positive that the condition $p \leq Y$ is equivalent to $p^2 \leq Y^2$ and we are able to define $Z$ without explicit use of square roots.)

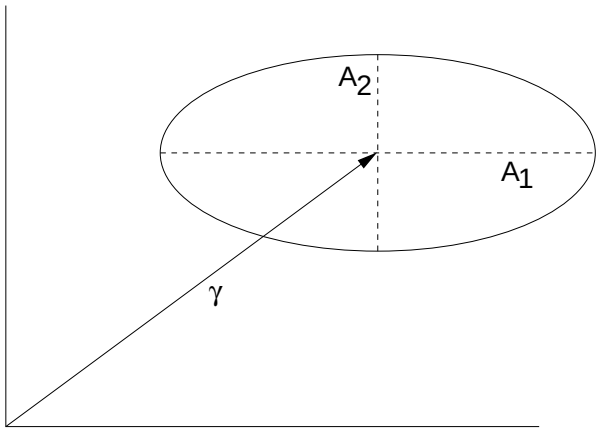


Figure 4.1: *Regions of constant von Mises stress are ellipsoids centered at locations* $\gamma$.

The integral of Eq. 4.3 is generally impossible to evaluate exactly, but approximate quadrature is straight-forward. Here we employ a numerical quadrature similar to the heuristic used in explaining Riemann integration.

## 4.3 Quadrature by Boxes

One of the few domain types over which we can integrate Gaussian distributions is boxes in $N$ space. Let $B_\lambda$ be one such box, then

$$\int_{B_\lambda} \prod_{r=1}^{N_P} \rho_r(y_r)\, dy_r = \prod_{r=1}^{N_P} \left[\Phi(y_{r,\max}) - \Phi(y_{r,\min})\right], \tag{4.6}$$

where $y_{r,\max}$ and $y_{r,\min}$ define the boundaries of $B_\lambda$, and

$$\Phi(x) = \frac{1}{\sqrt{2\pi}} \int_{-\infty}^{x} \exp(-s^2/2)\, \mathrm{d}s. \tag{4.7}$$

Note that $\Phi(x) = (1/2)\left(1 + \mathrm{erf}(x/\sqrt{2})\right)$.

Because $Z(\{D\}, \gamma, Y_0, Y)$ is a convex volume, it is easy to devise sequences of sets of boxes that are fully contained in $Z(\{D\}, \gamma, Y_0, Y)$ but whose net volume converge to that of $Z(\{D\}, \gamma, Y_0, Y)$ from below. Similarly, it is straightforward to define sequences of sets all of which contain $Z(\{D\}, \gamma, Y_0, Y)$, and whose volumes converge to that of $Z(\{D\}, \gamma, Y_0, Y)$ from above.

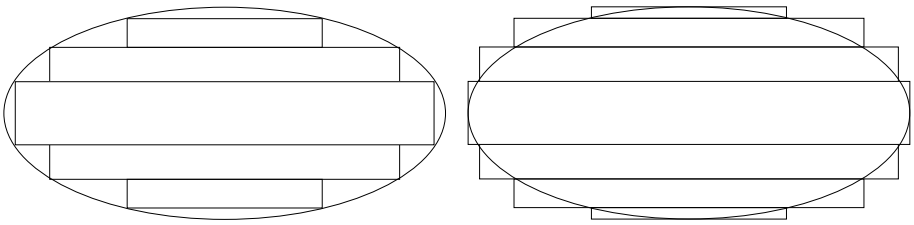

Figure 4.2: *Sets of boxes comprising subsets and supersets of the volume* $Z(\{D\}, \gamma, Y_0, Y)$ *for the case of* $N_P = 2$.

For the following examples, the above integration over $N$-dimensional ellipsoids was preformed via recursive calls to Matlab® function codes to obtain both upper and lower bounds for the integral. Listings can be found in Appendix D.

Credit should be given to Tibbits [8, 9] for creating approaches to the calculation of probability distribution for von Mises stress in the presence of pre-stress, but with some limitations. The approaches developed by Tibbits do not appear to accommodate the possibility of the number of random stress processes being less than the rank of the stress vector. The applications were limited to two dimensional problems where that assumption might more often be correct.

## 4.4 An Upper Bound for von Mises Probability

The recursive integrations associated with calculation of the probability distribution of von Mises stress where there are more than one random stress process present might be off-putting. Here we consider an obvious upper bound.

Let $B_U(\{D\}, \gamma, Y_0, Y)$ be the smallest $N$-box that entirely contains $Z(\{D\}, \gamma, Y_0, Y)$, that is

$$Z(\{D\}, \gamma, Y_0, Y) \subset B_U(\{D\}, \gamma, Y_0, Y). \tag{4.8}$$

The length of each side of the $B_U$ will be twice a semi-axis of $Z$. Because of Equation 4.8

$$\int_{Z(\{D\},\gamma,Y_0,Y)} \prod \rho_r(y_r)\,\mathrm{d}y_r \leq \int_{B_U(\{D\},\gamma,Y_0,Y)} \prod \rho_r(y_r)\,\mathrm{d}y_r$$
$$= \prod_{r=1}^{N_P} \left[\Phi(y_{r,\max}) - \Phi(y_{r,\min})\right], \quad (4.9)$$

where in this case $y_{r,\max}$ and $y_{r,\min}$ identify the coordinates at the corners of $B_U$.

## 4.5 Strategy for Implementation in a Finite Element Setting

Referring to Equations 4.3 and 4.4 and then backwards to Equations 3.25 and 3.29, we see that the necessary ingredients for computing the probability distribution at any location are $D(x)$, $G(x)$, and $\sigma_0(x)$.

The simplest strategy would be to implement the calculations, so much as possible, via post processing. The element variables $D$ and $G$ would come most naturally from a linear structural dynamics code, such as Salinas [4] or NASTRAN [2]. Because $D$ is diagonal and has at most 5 rows, the storage of it at each quadrature point is not an issue. Matrix $G$ has at most 5 rows and 6 columns, and storage space at each quadrature point should be quite manageable. Salinas is mentioned specifically because it lends itself to modification by the author and MSC NASTRAN is mentioned because of its DMAP capability [1]. The static stresses, $\sigma_0$ - and there might be ensembles of them - can come from a linear or nonlinear quasi-static analysis code.

There are a few more considerations:

- One caveat in employing results from different finite element codes is the requirement that the meshes and coordinate systems must be identical. Additionally, conventions on stress orientation must be the same.
- The ordering or rows of $D$ and $G$ should be that of the development above: diagonal terms of $D$ in decreasing order and each row of $G$ as defined in Equation 3.26.
- Because it is likely that $D$ will be stored as a 5x1 vector and $G$ will be stored as a 5x6 matrix, regardless of how many stress processes actually exist at the corresponding quadrature point, it would be helpful to store $N_P(x)$, the number of stress processes as well.

# 5 Example Problems

### Example Problem 1

Consider the simply supported beam shown in Figure 5.1, consisting of a beam subject to a static compressive load $F_0$ applied longitudinally and two dynamic loads $F_1(t)$ and $F_2(t)$ applied laterally. Loads $F_1$ and $F_2$ are assumed independent, stationary Gaussian processes with zero mean. The beam will be of length $L$, width $2w$, density $\rho_B$, cross-sectional area $A_B$, and Young's modulus $E$.

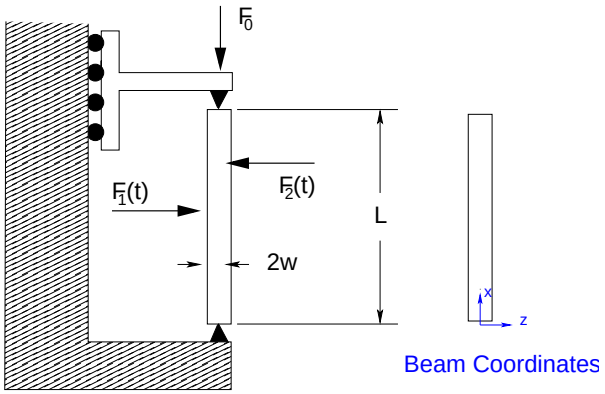


Figure 5.1: *Test case consisting of a simply supported beam of square cross section subject to a compressive longitudinal load $F_0$ and two random dynamic loads, $F_1(t)$ and $F_2(t)$ applied laterally.*

In general, each of $F_1$ and $F_2$ would excite many modes, but for the purpose of illustration, we we assume that the frequency content of $F_1$ is band limited so as to excite only the first bending mode and that the frequency content of $F_2$ is also band limited, but so as to excite only the second bending mode.

The static stress at any place on the beam is

$$\sigma_0 = \left\{ \begin{array}{c} -F_0/A_B \\ 0 \\ 0 \\ 0 \\ 0 \\ 0 \end{array} \right\} \tag{5.1}$$

with $F_0/A_B = 1$. For convenience with respect to expressing the stresses associated with the

bending modes, we assume that all constants are scaled such that

$$Ew\left(\frac{\pi}{L}\right)^2\sqrt{\left(\frac{2}{\rho_B A_B L}\right)}=1. \tag{5.2}$$

The stress due to bending of any mode $n \in (1,2)$ is

$$\Psi(x,z)=\left\{\begin{array}{cc} \sin\left(\frac{\pi x}{L}\right)\left(\frac{z}{w}\right) & 4\sin\left(\frac{\pi 2x}{L}\right)\left(\frac{z}{w}\right) \\ 0 & 0 \\ 0 & 0 \\ 0 & 0 \\ 0 & 0 \\ 0 & 0 \end{array}\right\} \tag{5.3}$$

where coordinates $x$ and $z$ are as indicated in Figure 5.1. Note that because the random loads generate only one component of stress ($\sigma_1$) we anticipate at most one random process to show up in the calculation of von Mises stress. Again, for purpose of illustration for this problem, we assume

$$\Gamma_{qq}=\left[\begin{array}{cc} 1 & 0 \\ 0 & 1/4 \end{array}\right] \tag{5.4}$$

The spatial distribution of RMS von Mises stress, that is, $p_{RMS}(x,z)$ defined by Eq. 3.10, is illustrated on the left of Figure 5.2. Also shown on the right side of the figure is $N_P(x,z)$, the rank of matrix $C(x,z)$ defined by Eq. 3.17, which describes the number of stress processes acting at that location. Because all of the modes associated with the random loads have nodal lines at the top, bottom and middle of the beam, there are no random processes at those locations.

The RMS von Mises stress might be considered a nominal stress level, but one is perhaps more concerned about the probability of von Mises stress reaching high levels. The cumulative distribution function for von Mises stress is given by Eq. 4.3. Suppose we are interested the 90th and 95th percentile of von Mises stress, that is, the values for Y such that the CDF defined by Equation 4.3 equals 0.9 and 0.95, respectively. Let $Y_{90}$ and $Y_{95}$ denote these values. The distributions of $90^{th}$ percentile and $95^{th}$ percentile von Mises stress are shown in Figure 5.3. The range of von Mises stress in Figure 5.3 is about twice that of the plot of RMS von Mises stress.

### Example Problem 2

Consider the cantilevered/simply supported beam shown in Figure 5.4, subject to a static compressive load $F_0$ applied longitudinally, random dynamic load $F_1(t)$ also applied longitudinally, and random dynamic load $F_2(t)$ applied laterally at the free end of the beam.

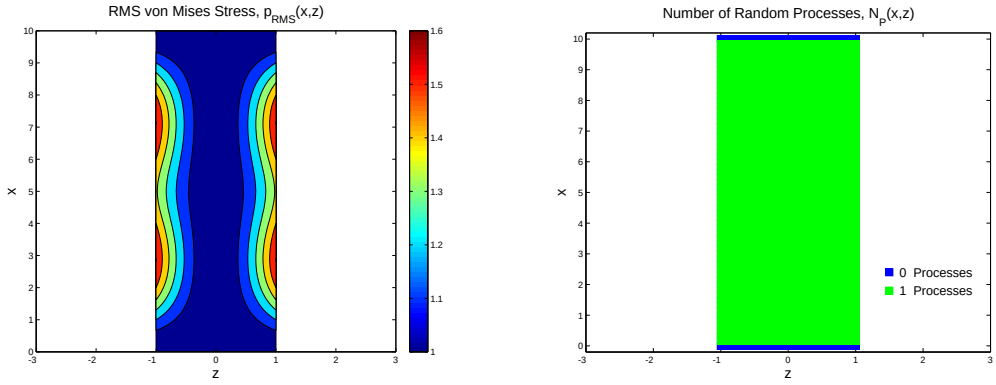


Figure 5.2: *The computed RMS von Mises stress resulting from the static pre-load and the lateral random dynamic loads is shown on the left. The distribution of the number of random processes is shown on the right.*

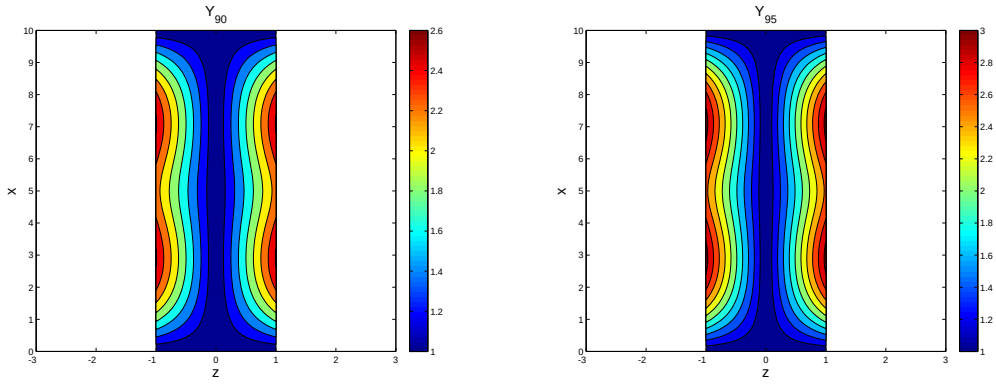


Figure 5.3: *The distribution of* $90^{th}$ *percentile and* $95^{th}$ *percentile von Mises stress are shown on the left and right contour plots, respectively.*

Loads $F_1$ and $F_2$ are assumed independent, stationary Gaussian processes with zero mean. The beam will be of length $L$, width $2w$, density $\rho_B$, cross-sectional area $A_B$, and Young's modulus $E$.

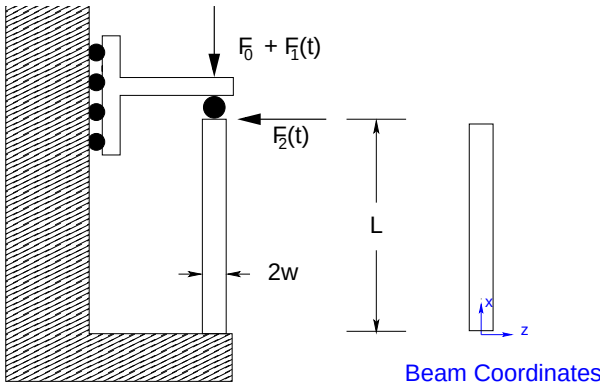


Figure 5.4: *Test case consisting of a cantilevered beam subject to a static compressive load $F_0$ applied longitudinally, random dynamic load $F_1(t)$ also applied longitudinally, and random dynamic load $F_2(t)$ applied laterally at the free end of the beam.*

We consider two axial modes excited by load $F_1$ and one bending load excited by $F_2$. Each of $F_1$ and $F_2$ excite many modes, but for the purpose of illustration, we associate the first two axial modes with $F_1$ and the first bending mode with $F_2$, and ignore the rest. Here we assume that the beam is sufficiently short so that shear stresses associated with that bending mode are significant.

Again, for convenience, we scale all constants such that Equation 5.2 holds, but this time to simplify the expression for stress associated with axial deformation. The first bending mode can be approximated by

$$u(x) = \frac{1}{24}\left(\frac{x}{L}\right)^2\left[\left(\frac{x}{L}\right)^2 - 4\left(\frac{x}{L}\right) + 6\right] \tag{5.5}$$

and we assume that that the geometric features permit the scaling of bending stress shown below. The matrix of modal stresses is given by

$$\Psi(x,z) = \left\{ \begin{array}{ccc} \frac{1}{2}\cos\left(\frac{\pi x}{2L}\right) & \frac{3}{2}\cos\left(\frac{\pi 3x}{2L}\right) & \frac{1}{2}\left[1-\left(\frac{x}{L}\right)^2\right]-\left(\frac{x}{L}\right)\left[1-\left(\frac{x}{L}\right)\right]\ \frac{z}{w} \\ 0 & 0 & 0 \\ 0 & 0 & 0 \\ 0 & 0 & \beta\left[1-\left(\frac{x}{L}\right)\right]\left(1-\left(\frac{z}{w}\right)^2\right) \\ 0 & 0 & 0 \\ 0 & 0 & 0 \end{array} \right\} \tag{5.6}$$

where $\beta = I_B/(2Lw_BA_B)$, which for this example we set to 1/2.

The static stress at any place on the beam is again

$$\sigma_0 = \left\{ \begin{array}{c} -F_0/A_B \\ 0 \\ 0 \\ 0 \\ 0 \\ 0 \end{array} \right\} \tag{5.7}$$

where $F_0/A_B = 1$. Again, for purpose of illustration for this problem, we assume a simple form for $\Gamma_{qq}$:

$$\Gamma_{qq} = \left[ \begin{array}{ccc} 1 & 0 & 0 \\ 0 & 1 & 0 \\ 0 & 0 & 3 \end{array} \right] \tag{5.8}$$

The RMS von Mises stress distribution for this case is shown on the left of Figure 5.5 and the distribution of the number of random processes is shown on the right side of that figure. Because all of the vibration modes associated with the random loads have nodal lines at the top of the beam, there are no random processes there. On the left and right sides of the beam, there are only axial stress components, so there can be at most one process. In the interior of the beam, there are axial stress components due to the axial modes and the bending mode and there is a shear component associated with the bending, making two random stress processes possible.

Again, we are interested in the RMS von Mises stress, but more concerned about the probability of von Mises stress reaching high levels. The cumulative distribution function (CDF) for von Mises stress defined by Equation 4.3 are illustrated by Figure 5.6 for locations 1 and 2. For the case of a single random stress process (such as location 2), the upper bound as described by Equation 4.9 is exact. More of the character of these distributions are indicated by the Probability Density Functions (PDF) shown in Figure 5.7 for locations 1 and 2 noted in Figure 5.5. The PDF for location 1 has a shape typical where there are two

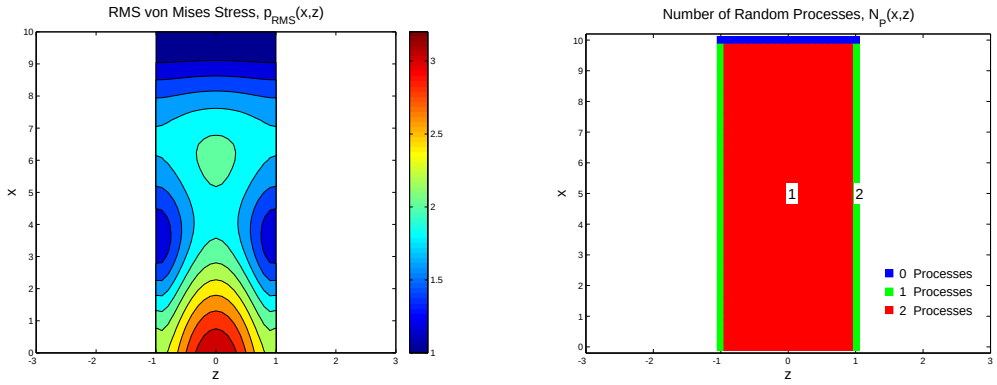


Figure 5.5: *The computed RMS von Mises stress resulting from the static pre-load and the lateral random dynamic loads is shown on the left. The distribution of the number of random processes is shown on the right. The locations marked "1" and "2" are discussed below.*

random stress processes and the PDF for location 2 has a shape typical where there is only one random stress process[7].

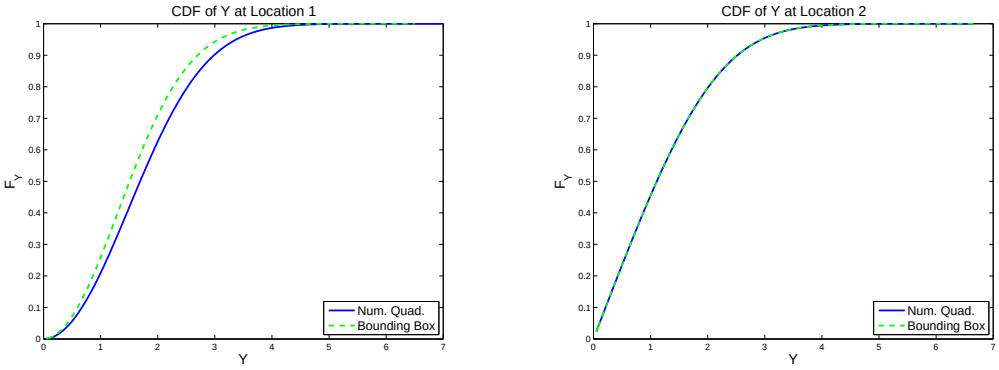


Figure 5.6: *The cumulative distribution functions (CDF) of von Mises stress at locations 1 and 2 are shown on the left and right, respectively. Also shown are upper bounds obtained via Equation 4.9. For the case of a single random stress process (such as location 2), the upper bound is exact.*

The spatial distributions of $5^{th}$ percentile, $50^{th}$ percentile, and $95^{th}$ percentile von Mises stress are shown in Figure 5.8. As expected, the range of von Mises stress in the $95^{th}$ percentile plot (right side of Figure 5.8) is substantially larger than those of the plot of RMS von Mises stress. The $5^{th}$ percentile plot is particularly interesting; because the random loads excite vibration that result in stresses that are co-linear with the static stresses, there

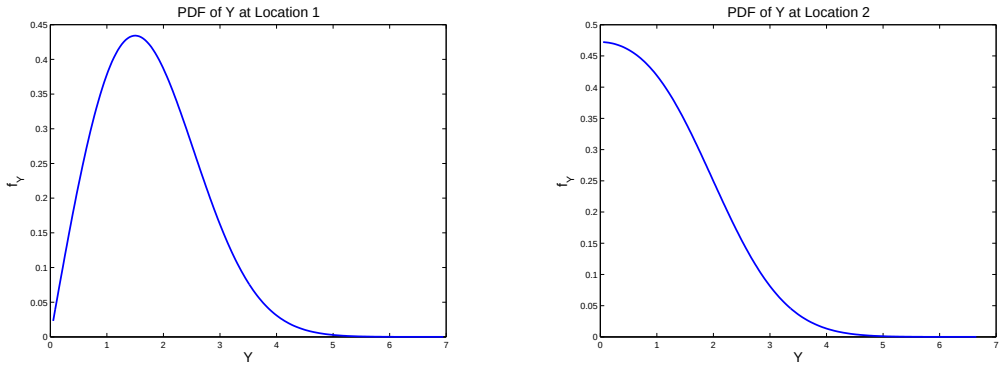


Figure 5.7: *The probability density functions (PDF) of von Mises stress at locations 1 and 2 are shown on the left and right, respectively.*

will be occasion when the random stresses act in direction opposite to the static stresses resulting in von Mises stresses less than that associated with the static loads alone. The plot of $50^{th}$ percentile von Mises stress is very different from the RMS von Mises stress; this is the difference between the square root of the time average of a quadratic or a random variable, and the median of the absolute value of that variable.

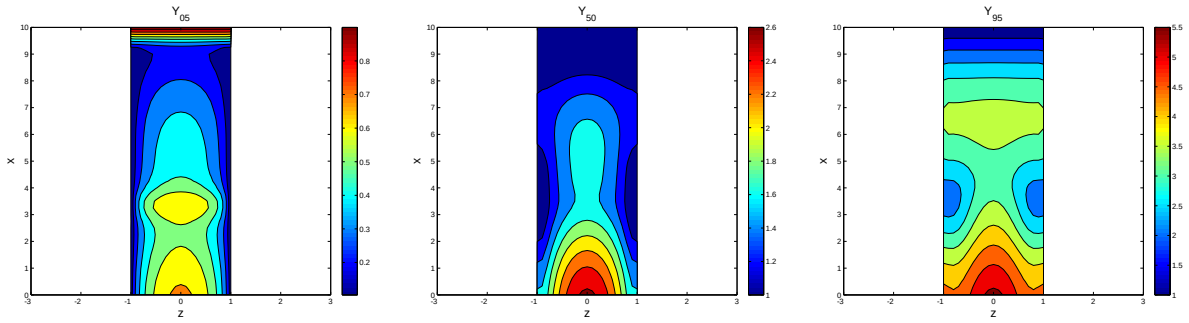


Figure 5.8: *The distribution of* $5^{th}$ *percentile,* $50^{th}$ *percentile, and* $95^{th}$ *percentile von Mises stress are shown on the left, middle, and right contour plots, respectively.*

# 6 Summary

The necessity of considering the von Mises stress (effective stress) in cases of random vibration is long known. Incorporating predictive mechanics of random vibration into modern engineering decision making requires expressing the stress response in a probabilistic manner. Though some progress in this direction has been reported in the literature, there are serious gaps with respect to the technology necessary to address random vibrations under preload - such as the vibration of decelerating space structures in atmospheric re-entry.

A significant improvement in capability is presented here. With the use of the standard elements of random vibration analysis (cross spectral density matrix of loads, the modal frequency response matrices, assumption of a stationary and Gaussian load, etc.), a formulation is presented to express the probability distribution of von Mises stress at any location even for cases where the structure is subject to an arbitrary distribution of in situ stress.

The formulation is not complicated and implementation in a finite element context would appear to be straightforward. On the other hand, evaluation of the necessary integrals can be compute intensive. A preferred implementation might involve the initial calculation of the full field of RMS von Mises stress and then calculation of the probability distribution of von Mises stress only at the "hot spots".

# References


[1] D. Bella and M. Reymond. *MSC/NASTRAN DMAP Module Dictionary*. MacNeal–Schwendler, Los Angeles, CA, 1997.

[2] R.S. Lahey, M.P. Miller, and M. Reymond. *MSC/NASTRAN Reference Manual, Version 68*. The MacNeal-Schwendler Corporation, 1994.

[3] John W. Miles. On structural fatigue under random loading. *Journal of the Aeronautical Sciences*, 21(11):753–762, November 1954.

[4] Garth Reese, Manoj K. Bhardwaj, and Timothy Walsh. Salinas theory manual. Sandia report SAND2004-4079, Sandia National Laboratories, PO Box 5800, Albuquerque, NM 87185, August 2004.

[5] J.B. Roberts and P.D. Spanos. *Random vibration and statistical linearization*. Dover Publications, 2003.

[6] Daniel J. Segalman, Clay W. G. Fulcher, Garth M. Reese, and Richard V. Field. An efficient method for calculating r.m.s. von Mises stress in a random vibration environment. *Journal Of Sound And Vibration*, 230(2):393–410, Feb 17 2000.

[7] Daniel J. Segalman, Garth M. Reese, Richard V. Field, and Clay W. G. Fulcher. Estimating the probability distribution of von Mises stress for structures undergoing random excitation. *Journal Of Vibration And Acoustics-Transactions Of The ASME*, 122(1):42–48, January 2000.

[8] Patrick A. Tibbits. Application of algorithms for percentiles of von mises stress from combined random vibration and static loadings. *Journal of vibration and acoustics*, 133(4):x, 2011.

[9] Patrick A. Tibbits. Percentiles of von mises stress from combined random vibration and static loading by approximate noncentral chi square distribution. *ASME Journal of Vibration and Acoustics*, 134(4):41009, 2012.

# A Evaluation of the Cross-Spectral Density Matrix for Modes

Much of the development of the method depends on evaluation of $\Gamma_{qq}$. This employs the modal frequency response matrix

$$\hat{q}(\omega) = H_q(\omega)\,\hat{F}(\omega), \tag{A.1}$$

where $\hat{q}(\omega)$ is the Fourier transform of modal displacement $q(t)$ and $\hat{F}(\omega)$ is the Fourier transform of the vector of forces $F(t)$.

The cross-spectral density matrix for the modal displacement is

$$S_{qq}(\omega) = \overline{H_q(\omega)}\,S_{FF}(\omega)\,H_q(\omega)^T \tag{A.2}$$

and it follows that

$$\Gamma_{qq} = \int_{-\infty}^{\infty} S_{qq}(\omega)\,\mathrm{d}\omega = \int_{-\infty}^{\infty} \overline{H_q(\omega)}\,S_{FF}(\omega)\,H_q(\omega)^T\,\mathrm{d}\omega. \tag{A.3}$$

# B Equivalence of Gaussian Random Vectors

We recall that the statistical characterization of Gaussian random vectors is completely specified by the vector of component means and by the matrix of covariance of the vector components. From Equation 3.13,

$$\beta(t) = X^{-1} Q^T q(t). \tag{B.1}$$

Because each element of the vector $q$ has zero mean, so must each component of $\beta$. Let us define

$$\tilde{q}(t) = Q\, Q^T\, q(t). \tag{B.2}$$

By reasoning similar to that above, each component of $\tilde{q}$ also has zero mean.

Next we evaluate

$$\begin{aligned} E\left[\tilde{q}(t)\,\tilde{q}(t)^T\right] &= Q\, Q^T\, E\left[q(t)\, q(t)^T\right]\, Q\, Q^T = Q\, Q^T \left(Q\, X\, Q^T\right) Q\, Q^T \\ &= Q\, X\, Q^T = \Gamma_{qq} = E\left[q(t)\, q(t)^T\right] \end{aligned} \tag{B.3}$$

which demonstrates that the covariance matrices of $q(t)$ and $\tilde{q}(t)$ are identical at any fixed time $t$. Because $q$ and $\tilde{q}$ are both Gaussian with zero mean and identical covariances, they are equivalent random vectors.

# C Evaluation of Equation 4.1

Let's integrate Equation 4.1 (repeated here for convenience) for the expected value of the square of the von Mises stress

$$E[p^2(t,x)] = \int_{-\infty}^{\infty} \cdots \int_{-\infty}^{\infty} \Big( (y(t)-\gamma(x))^T D(x)^2 (y(t)-\gamma(x)) + Y_0(x)^2 \Big) \prod_r \rho_r(y_r)\, \mathrm{d}y_r, \quad \text{(C.1)}$$

where $\rho_r$ is the density function of the standard Gaussian random variable. We first expand the quantity within the large parentheses

$$\begin{aligned} &\Big( (y(t)-\gamma(x))^T D(x)^2 (y(t)-\gamma(x)) + Y_0^2(x) \Big) \\ &\qquad = \big[ Y_0(x)^2 + \gamma(x)^T D(x)^2 \gamma(x) \big] + 2\, y(t)^T D(x)^2 \gamma(x) + y(t)^T D(x)\, y(t) \quad \text{(C.2)} \end{aligned}$$

The first term (in brackets) on the left hand side is a constant and can be factored out of the integral. The second term is odd in each component of $y$ so the integral involving it is zero. The third term requires more attention:

$$\begin{aligned} &\int_{-\infty}^{\infty} \cdots \int_{-\infty}^{\infty} y^T(t)\, D(x)\, y(t) \prod_r \rho_r(y_r)\, \mathrm{d}y_r \\ &\qquad = \int_{-\infty}^{\infty} \cdots \int_{-\infty}^{\infty} \left( \sum_r y_r(t)^2\, D_r(x)^2 \right) \prod_j \rho_j(y_j)\, \mathrm{d}y_j \\ &\qquad = \sum_r \left( \int_{-\infty}^{\infty} y_r(t)^2\, D_r(x)^2\, \rho_r(y_r)\, \mathrm{d}y_r \right) \prod_{j \neq r} \int_{-\infty}^{\infty} \rho_j(y_j)\, \mathrm{d}y_j = \sum_r D_r(x)^2, \quad \text{(C.3)} \end{aligned}$$

where we have used that

$$\int_{-\infty}^{\infty} \rho(y)\, \mathrm{d}y = \int_{-\infty}^{\infty} y^2\, \rho(y)\, \mathrm{d}y = 1. \quad \text{(C.4)}$$

Upon combining the non-zero terms and referring to Equation 3.29, we obtain Equation 4.1.

# D Recursive Functions to Evaluate the Probability Integral

The following listings are of Matlab® recursive function codes to obtain both upper and lower bounds for the integral of Equation 4.3 over the $N$-dimensional ellipsoid $Z(\{D\}, \gamma, Y_0, Y)$.

12/27/12 11:18 PM /Use.../EvalPBelow.m 1 of 1

```
function P = EvalPBelow( gamma, D, Z, Nint)
% Recursive routine to perform probability integral
% (y-\gamma)^T D^2 (y - \gamma) < Y^2 -Y_0^2
%
% In initial call, P=EvalPBelow(gamma, D, Y^2-Y-^2, Nint)
% Nint is the number of intervals in each dimension
%
A = Z/D(1);
r2 = sqrt(2);

if length(D)==1   % this is the last interval
    ymax = gamma(1)+A;  ymin=gamma(1)-A;
    P = (1/2)*( erf(ymax/r2) - erf(ymin/r2) );
else
    % perform the integration over multiple dimensions
    dy = 2*A/Nint;
    span = linspace(-A+dy/2, A-dy/2, Nint+1);
    y = span + gamma(1);
    P = 0;
    for i=1:Nint
        yy = max(abs([span(i) span(i+1)]));
        ZZ = sqrt(Z^2 - (yy*D(1))^2);

        P = P + ...
             (1/2)*( erf(y(i+1)/r2) - erf(y(i)/r2) ) ...
             *EvalPBelow( gamma(2:end), D(2:end), ZZ, Nint);
    end
end
```

Figure D.1: *A recursive function to approximate the integral in Equation 4.3 from below. This involves performing exact integration on a set of $N$-dimensional boxes entirely contained in the ellipsoid $Z(\{D\}, \gamma, Y_0, Y)$.*

```
function P = EvalPAbove( gamma, D, Z, Nint)
% Recursive routine to perform probability integral
% (y-\gamma)^T D^2 (y - \gamma) < Y^2 -Y_0^2
%
% In initial call, P=EvalPBelow(gamma, D, Y^2-Y-^2, Nint)
% Nint is the number of intervals in each dimension
%
A = Z/D(1);
r2 = sqrt(2);

if length(D)==1   % this is the last interval
    ymax = gamma(1)+A;  ymin=gamma(1)-A;
    P = (1/2)*( erf(ymax/r2) - erf(ymin/r2) );
else
    % perform the integration over multiple dimensions
    dy = 2*A/Nint;
    span = linspace(-A, A, Nint+1);
    y = span + gamma(1);
    P = 0;
    for i=1:Nint
        yy = min(abs([span(i) span(i+1)]));
        ZZ = sqrt(Z^2 - (yy*D(1))^2);

        P = P + ...
             (1/2)*( erf(y(i+1)/r2) - erf(y(i)/r2) ) ...
             *EvalPAbove( gamma(2:end), D(2:end), ZZ, Nint);
    end
end
```

Figure D.2: *A recursive function to approximate the integral in Equation 4.3 from above. This involves performing exact integration on a set of $N$-dimensional boxes which entirely contain the ellipsoid $Z(\{D\}, \gamma, Y_0, Y)$.*

# DISTRIBUTION:

| | | |
|---|---|---|
| 1 | MS 0346 | Clark R. Dohrmann, 01542 (electronic copy) |
| 1 | MS 0346 | D. Gregory Tipton, 01523 (electronic copy) |
| 1 | MS 0346 | Diane E. Peebles, 01526 (electronic copy) |
| 1 | MS 0346 | Michael A. Guthrie, 01523 (electronic copy) |
| 1 | MS 0346 | Michael J. Starr, 01526 (electronic copy) |
| 1 | MS 0346 | Michael Ross, 01523 (electronic copy) |
| 1 | MS 0346 | Mikhail Mesh, 01523 (electronic copy) |
| 1 | MS 0346 | Richard V. Field, 01526 (electronic copy) |
| 1 | MS 0346 | Wil A. Holzmann, 01523 (electronic copy) |
| 1 | MS 0372 | Chi S. Lo, 01524 (electronic copy) |
| 1 | MS 0372 | Kenneth W. Gwinn, 01524 (electronic copy) |
| 1 | MS 0380 | Garth M. Reese, 01542 (electronic copy) |
| 1 | MS 0380 | Joseph Jung, 01542 (electronic copy) |
| 1 | MS 0386 | Timothy S. Edwards, 01527 (electronic copy) |
| 1 | MS 0431 | John Pott, 00511 (electronic copy) |
| 1 | MS 0557 | Brandon Zwink, 01522 (electronic copy) |
| 1 | MS 0557 | Darrick M. Jones, 01521 (electronic copy) |
| 1 | MS 0557 | David Epp, 01522 (electronic copy) |
| 1 | MS 0557 | Eric C. Stasiunas, 01521 (electronic copy) |
| 1 | MS 0557 | Fernando Bitsie, 01521 (electronic copy) |
| 1 | MS 0557 | Jerry W. Rouse, 01523 (electronic copy) |
| 1 | MS 0557 | Laura Jacobs, 01521 (electronic copy) |
| 1 | MS 0557 | Randall L. Mayes, 01522 (electronic copy) |
| 1 | MS 0557 | Todd W. Simmermacher, 01523 (electronic copy) |
| 1 | MS 0828 | Walter R. Witkowski, 01544 (electronic copy) |
| 1 | MS 0840 | Justine E. Johannes, 01500 (electronic copy) |
| 1 | MS 0942 | Wei-Yang Lu, 08256 (electronic copy) |
| 1 | MS 1070 | Matthew R. Brake, 01526 (electronic copy) |
| 1 | MS 9013 | James P. Lauffer, 08231 (electronic copy) |
| 1 | MS 9042 | Michael D. Jew, 08259 (electronic copy) |
| 1 | MS 9042 | Mike Chiesa, 08259 (electronic copy) |
| 1 | MS 9042 | Mary E. Gonzales, 08250 (electronic copy) |
| 5 | MS 9042 | Daniel J. Segalman, 08259 (electronic copy) |
| 1 | MS 0899 | Technical Library, 9536 (electronic copy) |

Sandia National Laboratories